Luminescence, spectroscopic and electrochemical studies on halogen-based thulium compound: TmCl₃

S. Shanmugha Soundare ^a, S. Ariponnammal ^b, R. Jayavel ^{a, *}

Rare earth thulium tri chloride (TmCl₃) has consistent distribution of brick shaped, rectangular particles with monoclinic crystal structure and 92 nm crystallite size. Density of dislocation is $1.181 \times 10^{14} \text{m}^{-2}$. The calculated strain is 3.788×10^{-4} . The refractive index is 3.067, and the energy gap is 5.26 eV. Optical studies on TmCl₃ assigns energy level transitions. Low-temperature magnetic studies upto 20K have revealed intriguing phase transitions between 50 and 99K which may be paramagnetic to antiferromagnetic transition. Investigation of aqueous solution of TmCl₃ exhibits wider potential window 2.86V indicating electrochemically superior nature of the electrolyte.

(Received June 8, 2025; Accepted September 15, 2025)

Keywords: TmCl₃, SEM, XRD, Electrochemical analysis, Optical, Magnetic

1. Introduction

Lanthanide materials are the subject of the most research because of its use in astronomy, medicine, lasers, and remote sensing. The presence of a rare earth ion show broad, wide emission [1-5]. Appropriate rare earth ions that produce emission at a specific wavelength are used in the design of optical devices. Mid-IR pump lasers and medical applications have been found to use thulium [6, 7]. Thulium is a rarest rare earth metal [1-8]. A vivid blue luminescence is displayed by Tm³⁺ ions [2–9]. Thulium is used for laser manufacturing and for surgical purposes. Thulium is used in handheld x-ray machines as radiation source and in nuclear reactions. It is used in microwave devices [1-8]. When exposed to ultraviolet light, thulium fluoresces blue. Euro banknotes include thulium as a deterrent to counterfeiting [3–10]. Tm-doped calcium sulfate's blue fluorescence has been utilized in personal dosimeters to visually monitor radiation exposure [2–9]. The production of effective electricity-generating windows based on the luminescent solar concentrator uses Tmdoped halides.[4-11]. Thulium with atomic number 69 has +3 oxidation state in halides, oxides and other substances. The +2 oxidation state of thulium is likewise stable [12]. The magnetic property of rare earths depends on 4f shell electrons [13]. Thulium remains a unique model object for fundamental studies on magnetic. It displays paramagnetism above 56 K, antiferromagnetism between 32 and 56 K, and ferromagnetism below 32 K [12]. Thulium chloride is used for the manufacturing of thulium compounds and chemical reagents [14]. It is a source of crystalline thulium soluble in water. When chlorides dissolved in water, it conducts electricity. Electrolysis decomposes compounds of chlorides into metal and gas of chlorine [15]. In addition to the evident possibilities of practical applications, Thulium finds commercial applications. Thulium is used in the creation of lasers. Stable Thulium-169 is served as a source of radiation in x-ray portable devices. It has potential usage in ceramic magnetic materials and ferrites in the equipment of microwaves. Calcium sulphate doped with Thulium finds usage in radiation dosimeters since its fluorescence register even for low levels [16]. It is also used in production of glass and some oxides of hightemperature superconductors [17]. Chlorides and acetates of rare earth are used in making waterproof and acid-resistant fabrics [18]. In addition, new areas of applications were recently demonstrated. During the synthesis of NaYF₄:Y/Tm upconversion nanocrystal hybrid structure

_

^a Centre for Nanoscience and Technology, Anna University, Chennai-600025, Tamilnadu, India

^b Department of Physics, Gandhigram Rural Institute, Deemed To Be University, Gandhigram-624 302, Dindigul District, Tamilnadu, India

^{*} Corresponding author: rjvel@annauniv.edu https://doi.org/10.15251/DJNB.2025.203.1125

semiconductor finds application in enhanced near infra-red photocatalysis [19]. Thulium chloride has numerous applications in the field of lasers, phosphors, glass, ceramics, and doping agents for amplifiers of fiber. Motivated by these applications, thulium chloride is studied and reported.

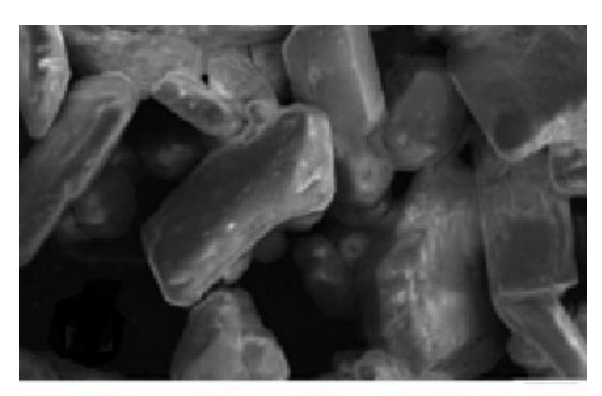
2. Methods

TmCl₃, a rare earth white color compound as powder, as synthesized from alfa aesar is characterized. The structure of TmCl₃ sample was confirmed by PANalytical X'Pert Pro XRD diffractometer (XRD) using Cu Kα radiation. The EVO-18 model CAREL ZEISS made scanning electron microscope (SEM) recording. At the same time, the Perkin Elmer Lambda 35 spectrophotometer for Ultraviolet-Visible (UV–VIS) spectrum, the VARIAN Cary Eclipse Fluorescence spectrophotometer for luminescence (PL) spectrum, and the Perkin Elmer BX model spectrophotometer for Fourier transform infrared (FTIR) spectrum are used. A Lakeshore model VSM 7410 performs magnetic measurements in low temperatures. The Bio-Logic VSP potentiostat model was used for electrochemical measurements.

3. Results and discussions

3.1. Studies on surface morphology and structure

The SEM image (Figure 1) of TmCl₃ at 500× magnification reveals an intriguing morphology of uniformly dispersed, almost rectangular brick-shaped particles. Figure 2 displays the TmCl₃ XRD pattern. By using the least-square-fit approach, cell characteristics are ascertained and the peaks are indexed.



⊢ 20µm Mag=500x EHT=10 kV

Fig. 1. SEM image of TmCl₃.

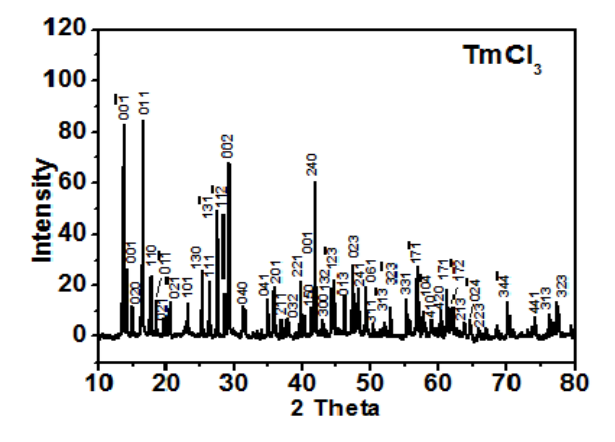


Fig. 2. XRD pattern of TmCl₃.

TmCl₃ is crystallized in monoclinic structure. The lattice parameters are $6.786\pm0.01\text{Å}$, b=11.730±0.01Å, c=6.399±0.02Å, α = γ =90°, β =110.5°, V=477.1ų. These agree with ASTM file 35-1413. The size of the crystallite, determined by XRD, is 92nm, by Scherrer equation [20-22]. The density of dislocation is 1.181 \times 10¹⁴ m⁻². There is 3.788×10⁻⁴ strain [20-22]. The crystal parameters deduced from the XRD data for TmCl₃ are shown in Table 1.

Sl.No	2θ	d (Å)	I/I_0	hkl	Sl.No	2θ	d (Å)	I/I_0	hkl
1	13.726	6.4461	100.00	001	24	44.349	2.0409	8.44	132
2	14.233	6.2178	17.01	001	25	44.738	2.0241	9.40	123
3	15.094	5.8650	5.26	020	26	46.147	1.9655	5.58	013
4	16.596	5.3374	91.77	011	27	47.360	1.9179	14.35	023
5	17.787	4.9826	11.07	110	28	48.176	1.8874	7.83	241
6	18.537	4.7827	4.79	011	29	49.251	1.8486	6.74	061
7	19.799	4.4806	2.63	021	30	50.468	1.8069	0.87	311
8	20.473	4.3346	5.10	021	31	52.108	1.7538	1.54	313
9	23.118	3.8442	2.73	101	32	52.988	1.7267	3.36	323
10	25.336	3.5125	12.29	130	33	55.249	1.6613	4.59	331
11	26.401	3.3732	9.81	111	34	56.851	1.6182	12.90	$17\overline{1}$
12	27.579	3.2317	40.13	131	35	57.748	1.5952	1.70	$10\bar{4}$
13	28.606	3.1180	7.36	112	36	59.161	1.5604	0.83	410
14	29.154	3.0607	74.02	002	37	60.376	1.5319	3.09	420
15	31.565	2.8321	3.27	040	38	61.306	1.5109	6.67	171
16	35.010	2.5609	5.94	041	39	62.048	1.4946	2.20	172
17	35.837	2.5037	8.78	201	40	63.818	1.4573	0.58	213
18	36.913	2.4332	2.27	211	41	64.528	1.4430	2.41	$02\bar{4}$
19	37.648	2.3873	1.94	032	42	65.718	1.4197	1.09	223
20	39.671	2.2701	10.19	221	43	70.235	1.3391	4.64	$34\overline{4}$
21	41.250	2.1868	3.70	150	44	74.210	1.2769	3.20	441
22	41.860	2.1563	53.03	240	45	76.417	1.2454	2.34	313
23	42.979	2.1027	1.49	300	46	77.518	1.2304	4.55	323
Structure		a in Å	b in Å	c in Å	V in Å ³	Dislocation Density m ⁻²		Strain	
Monoclinic		6.786± 0.01	11.730 ±0.01	6.399 ±0.02	477.1	1.181× 10 ¹⁴		3.788× 10 ⁻⁴	

Table 1. XRD data for TmCl₃.

3.2. Optical studies

Figure 3 displays UV-VIS spectrum. In the UV zone, the absorption is high at roughly 208.2nm. $TmCl_3$ can, therefore, be employed as a filter in the UV range. Furthermore, a high transmittance is seen, with absorption peaks in the visible spectrum. The broad transmission range of $TmCl_3$ between 300 and 1100 nm makes it a viable candidate for use in the optoelectronic industry. The electron configuration of Tm^{3+} is $[Xe]4f^{12}$. It is an ion of infrared laser.

The absorption spectrum of trivalent Thulium has a peak at 357.8nm, which is closer to the third harmonic Nd: YAG laser pulsing at 355nm. The ground state ${}^{3}H_{6}$ absorption of ${}^{1}D_{2}$, ${}^{1}G_{4}$, ${}^{3}F_{2}$, ${}^{3}F_{3}$, ${}^{3}F_{4}$, and ${}^{3}H_{4}$ levels is represented by absorption peaks at 357.8, 465.6, 682.8, 702.4, 773.5, and 800.6 nm, respectively. ${}^{3}F_{4} \rightarrow {}^{1}G_{4}$ and ${}^{3}H_{5} \rightarrow {}^{1}G_{4}$ transitions are represented by 658.4 and 791.7nm absorption peaks, respectively [23-27].

The energy gap measured in Figure 4, which plots $(\alpha h \nu)^{1/2}$ against energy [28-30], is 5.26 eV. The Urbach energy is 0.1509 eV based on the Urbach plot (Figure 5). From optical energy gap, refractive index of 3.067 is derived using the relation,

$$\frac{n^2 - 1}{n^2 + 2} = 1 - \sqrt{\frac{E_{opt}}{20}} \tag{1}$$

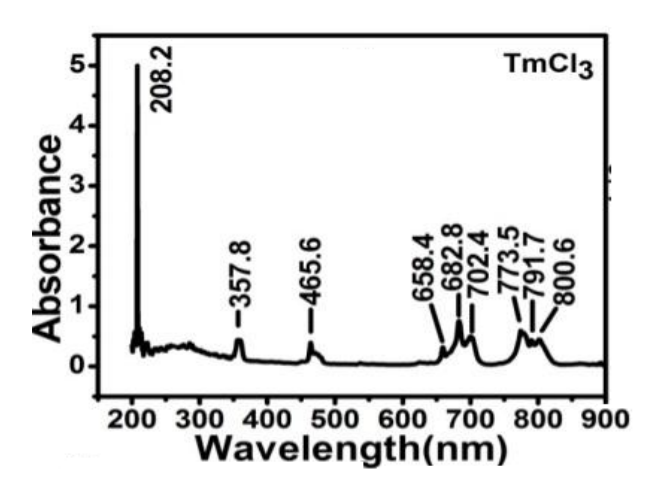


Fig. 3. UV-visible asorbance spectrum of TmCl₃.

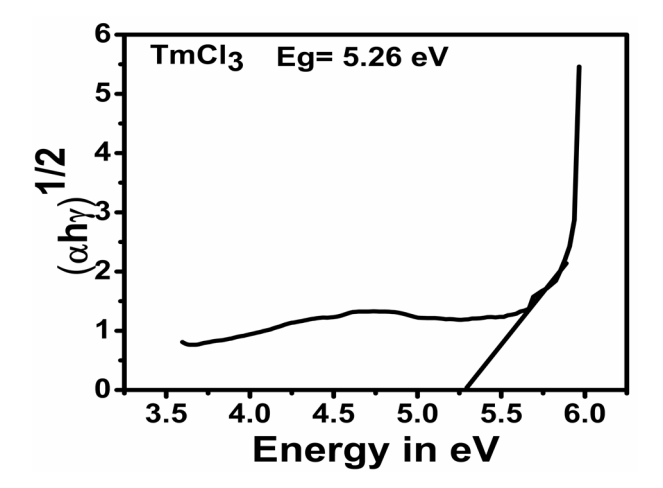


Fig. 4. $(\alpha hv)^{1/2}$ versus energy for $TmCl_3$.

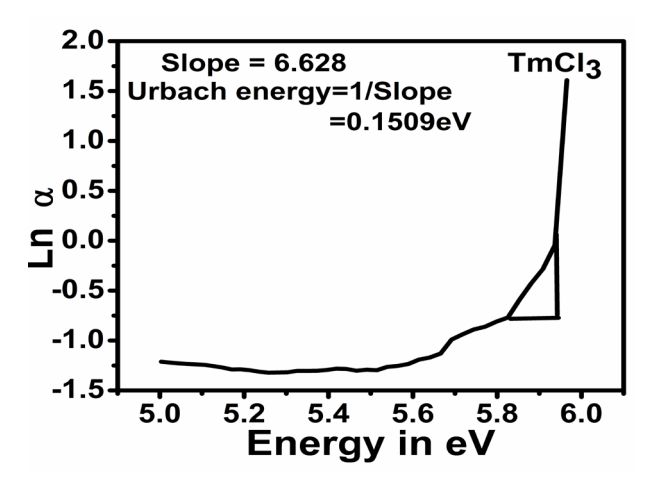


Fig. 5. Urbach plot of TmCl₃.

Figure 6 shows the emission spectrum of PL. with excitation wavelength 390nm. A strong UV emission (~388.3 nm), blue weak emission (~459.3 nm), and red moderate emission (~788.8 nm) corresponds to ${}^{1}D_{2} \rightarrow {}^{3}H_{6}$, ${}^{1}G_{4} \rightarrow {}^{3}H_{6}$ and ${}^{1}G_{4} \rightarrow {}^{3}H_{5}$ transitions [31].

Figure 7 displays the TmCl₃ FTIR spectrum. Assignments to absorption frequencies are shown in Table 2. The O—H bond is ascribed to the broad trough centered at 3364.4cm⁻¹, extending from 2722.7 to 3692.9 cm⁻¹[32-33]. This suggests the hygroscopic character of the material. Tm-Cl bonding corresponds to fingerprint region bands at 602.5 and 495.2cm⁻¹ [34].

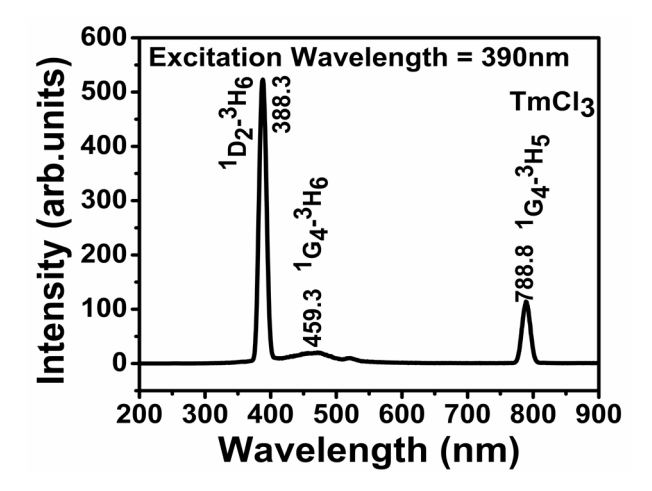


Fig. 6. PL Spectrum of TmCl₃.

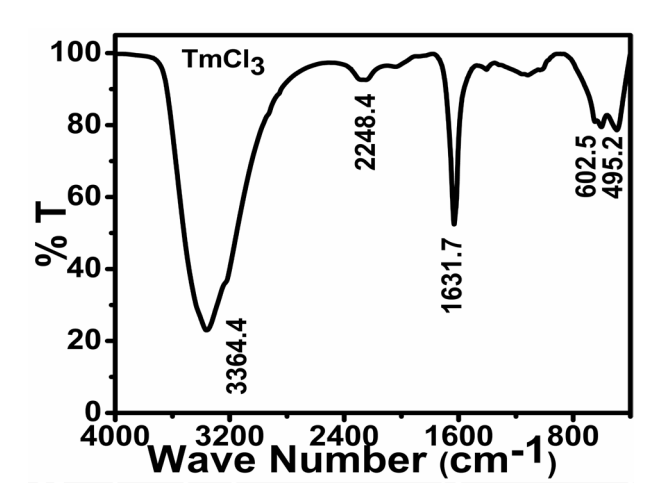


Fig. 7. FTIR of TmCl₃.

Table 2. FTIR assignment of TmCl₃.

Wave Number in cm ⁻¹	Assignment
3364.4	О-Н
2248.4	О-Н
1631.7	О-Н
602.5	Tm-Cl
495.2	Tm-Cl

3.3. Low temperature magnetic studies

According to reports, Thulium is ferromagnetic below 32 K, antiferromagnetic between 56 and 32 K, and paramagnetic beyond 56 K [35]. TmCl₃ demonstrates zero field cooled (ZFC) and field cooled (FC) characterization utilizing a vibrating sample magnetometer in Figure 8. They are both inherently reversible. Magnetic susceptibility decreases until it approaches saturation as temperature increases. In field cooling, 2000 Oe is the applied field that aligns almost all spins of Thulium and results almost crystal's magnetism saturation. As a result, there is cooperative contact between thulium spins. According to published literature, the ZFC and FC cooling curves exhibit some phase transition between 50 and 99K. This phase shift may be the result of a paramagnetic to antiferromagnetic transition [35-38]. The M-H curve of TmCl₃ at 300K in Figure 9 confirms the sample's paramagnetic composition.

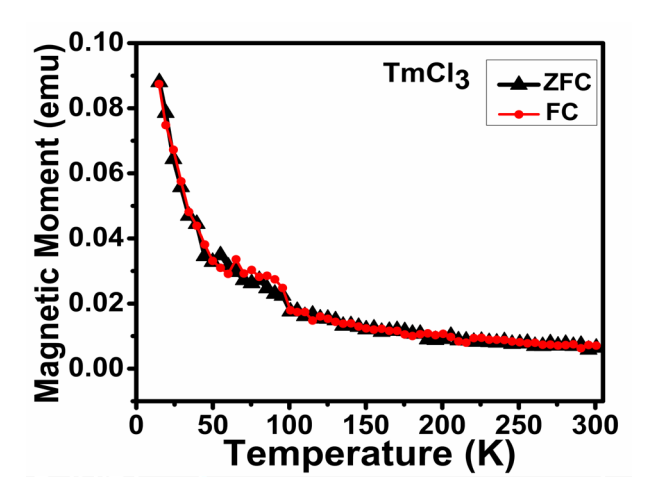


Fig. 8. ZFC and FC magnetic behavior of TmCl₃.

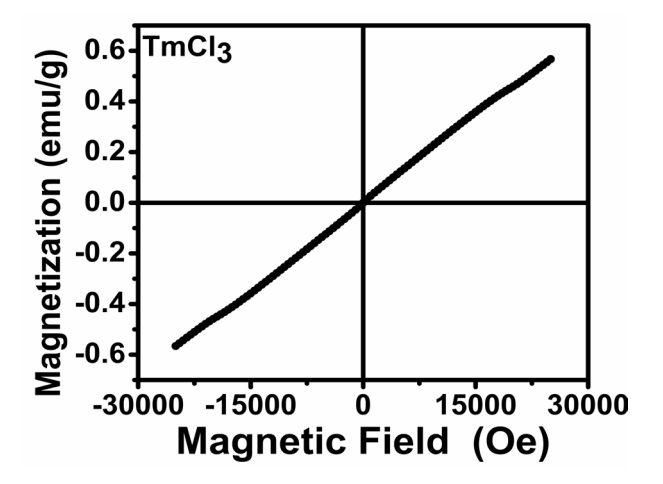


Fig. 9. M-H curve of TmCl₃.

3.4. Electrochemical analysis of electrolyte

Inorganic salts soluble in water are the greatest option for aqueous electrolytes utilized in most of the pseudocapacitors since they may be employed directly as electrodes and provide significant amount of free cations. The creation of innovative inorganic pseudocapacitors is fraught with difficulties. Certain materials used for pseudocapacitor electrodes had particular capacitance values that were higher than those predicted value. Typically, pseudocapacitors have shorter cycle

lives and lower energy densities[39]. According to reports, the issue with the ionic level can be resolved by creating water-soluble inorganic salt pseudocapacitors and using commercially available inorganic salts as an alkaline electrolyte's electrode materials [39]. Previous research has demonstrated that reactive cations in water-soluble inorganic salt pseudocapacitors can change into colloids [39]. These colloids contribute high responsiveness towards electrochemical redox processes.

Considering their electrochemical properties, aqueous electrolytes are more versatile than non-aqueous solvents in terms of their uses. However, they are hampered by quick water electrolysis in aqueous electrolytes, creating small potential window. The thermodynamic potential window of 1.23V for water is well known. Potential window width is an essential parameter in the field of capacitors. Capacitors, which employ aqueous electrolytes, should go hand in hand with potential window extension. The cyclic voltammogram measures the electrochemical performance of TmCl₃ nanoparticle electrolytes by system with three electrodes. The reference electrode is a saturated calomel electrode, and the counter electrode is a platinum (Pt) plate. Glassy carbon is an active electrode. An electrolyte solution containing 1 milligram TmCl₃ in ten milliliters double-distilled water is utilized.

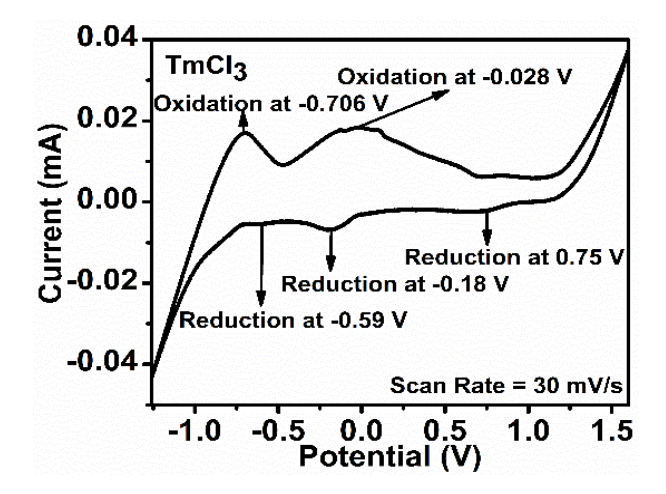


Fig. 10. Cyclic voltammogram of TmCl₃ in electrolyte.

By using cyclic voltammogram, the electrolyte shows the broadest potential window of 2.86V, ranging from -1.26V to 1.6V (Fig.10). It attests to its superior electrolyte composition, making it suitable for a greater potential range of possible device uses. Figure 10 shows a TmCl₃ cyclic voltammogram at 30mV/s scan rate. It exhibits characteristic oxidation peaks at -0.706V and -0.028V, corresponding to Tm²⁺ and Tm³⁺ ion indicating pseudocapacitive behavior [40-42]. Due to the Tm³⁺ contribution, three reduction peaks were detected at 0.75V, -0.18V, and -0.59V. It shows the irreversible process brought on by the electron transfer process. The CV curve's area is 6.1749E-5. The computed specific capacitance is 360mF/g.

3.5. Impedance analysis

Nyquist graph of TmCl₃ is depicted in Figure 11 to understand electron transfer process. It displays two half-circles. One shows a large semicircle of charge transfer resistance (8.838 Ω) and series resistance (Rs. 1.148 Ω), suggesting a significant contribution from charge transfer resistance [43–46]. Another extremely small semicircle with charge transfer resistance Rct 0.812 Ω and series resistance Rs 0.445 Ω is depicted as extended inset by arrow. Figure 11's inset displays the equivalent Randles circuit model for the Nyquist plot. When both diffusion and kinetics are important, it can be applied to explain processes at the electrode [46].

The Warburg element, or ZWAR, which contains species diffusion coefficient data, is made up of a double-layer capacitor C, solution resistance ($R\Omega$), and charge transfer resistance. The Warburg impedance (Figure 11) shows a 45° sloping straight line under semi-infinite conditions. [47-48]. Strong contribution of charge transfer resistance is seen in big circles in impedance analysis, which aligns with CV studies.

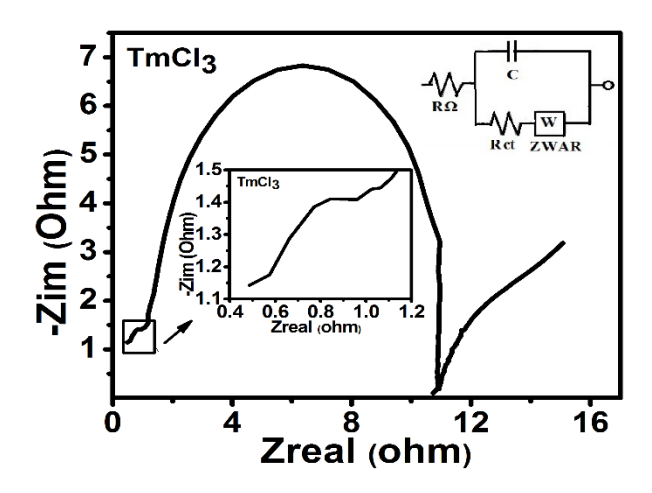


Fig. 11. Nyquist Plot for TmCl₃.

4. Conclusions

Brick-shaped particles with a homogeneous distribution are present in trivalent Thulium chloride. Lattice parameters are a=6.786±0.01Å, b=11.730±0.01Å, c=6.399±0.02Å, α = γ =90°, β =110.5°, and V=477.1ų, confirms monoclinic structure. The size of the crystallite is 92nm. Density of dislocation is 1.181 × 10¹⁴m⁻². The calculated strain is 3.788 × 10⁻⁴. According to a cyclic voltammetry investigation, an aqueous solution of TmCl₃ was found to have a widest potential window 2.86V indicating that it was electrochemically superior. It was observed that TmCl₃ pseudocapacitor electrodes in alkaline electrolytes underwent a crystallization change. Chemical coprecipitation and faradaic redox processes were used to crystallize the electrochemically reactive colloids. According to impedance study, the charge transfer resistance is 8.838 Ω , and series resistance Rs is 1.148 Ω . As a result, TmCl₃ presents itself as a viable rare earth electrode material for use in supercapacitors. Energy gap is deduced as 5.26eV. Low temperature magnetic studies on TmCl₃ show paramagnetic behavior at room temperature with interesting phase transitions between 50 and 99K.

Acknowledgments

The authors are grateful to DST-FIST, Department of Physics, Gandhigram Rural Institute, Deemed To Be University, Gandhigram, Tamilnadu, India, for providing XRD facilities, and to SAIF-IITM, Chennai, India, for granting access to the magnetic research.

References

[1] D. Zhou, D. Jin, Q. Ni, X. Song, X. Bai, K. Han, J. Am. Cer. Soc. **102**, 4748 (2019); https://doi.org/10.1111/jace.16361

[2] Y. Chu, Y. Yang, Y. Liu, S. Wang, C. Shi, D. Zhang, H. Li, J. Peng, N. Dai, J. Li, L. Yang, J. Non-Cryst. Sol. **529**, 119704 (2020); https://doi.org/10.1016/j.jnoncrysol.2019.119704

- [3] A. Kaur, A. Khanna, M. Gonzalez-Barriuso, Fernando Gonzalez, J. Mater. Sci.:Mater. Electron. **32**, 17266 (2021); https://doi.org/10.1007/s10854-021-06228-3
- [4] L.M. Marcondes, L. Rodrigues, C.R. Da Cunha, R.R. Goncalves, A.S.S. De Carmargo, F.C. Cassanjes, G.Y. Poirier, J. Lumin. **213**, 224 (2019); https://doi.org/10.1016/j.jlumin.2019.05.012
- [5] K. Annapoorani, N. Suriyamurthy, T.R. Ravindra, K. Marimuthu, J. Lumin. **171**, 19 (2016); https://doi.org/10.1016/j.jlumin.2015.10.071
- [6] N. Elkhoshkhany, S. Marzouk, M. El-Sherbiny, S. Yousri, M.S. Alqahtani, H. Algarni, M. Reben, El Sayed Yousef, Res. Phys. **14**, 104202 (2021); https://doi.org/10.1016/j.rinp.2021.104202
- [7] Y. Xu, Y. Tian, Q. Liu, X. Sheng, W. Tang, J. Zhang, S. Xu, J. Lumin. **211**, 418 (2019); https://doi.org/10.1016/j.jlumin.2019.04.011
- [8] https://en.wikipedia.org/wiki/Thulium
- [9] Emsley, John, US: Oxford University Press. pp. 442–443 (2001)
- [10] Wardle, Brian, A John Wiley & Sons, Ltd., Publication, p. 75 (2009)
- [11] O.M.En Kate, K.W.Krämer, E.Van der Kolk, Solar Energy Materials and Solar Cells, **14**, 115 (2015); https://doi.org/10.1016/j.solmat.2015.04.002
- [12] https://www.rsc.org/periodic-table/element/69/thulium
- [13]S.Ariponnammal, S.Shalini, S. Anusha, Cryst. Res. Technol. **57**, 2200106 (2022);. https://doi.org/10.1002/crat.202200106
- [14] https://www.aemree.com/thulium-chloride.html
- [15] https://www.samaterials.com/thulium/1535-thulium-chloride.html
- [16] https://www.lenntech.com/periodic/elements/tm.html
- [17] https://study.com/academy/lesson/thulium-uses-facts-properties.html
- [18] https://www.priyamstudycentre.com/2021/03/rare-earth-element.html
- [19] L.M.Jin, X.Chen, C.K.Siu, F.Wang, S.F.Yu, ACS Nano, **11**, 843 (2017); https://doi.org/10.1021/acsnano.6b07322
- [20]S.Ariponnammal, S.Anusha Mater. Today. Proc., **66**, 1606 (2020); https://doi.org/10.1016/j.matpr.2022.05.248
- [21] Are crystallite size and particle size are the same?
- https://www.researchgate.net/post/Are crystallite size and particle
- [22] S. Ariponnammal, S. Shalini, S. Nishadini Devi, Mater. Today Proc. **35**, 39 (2021); https://doi.org/10.1016/j.matpr.2019.05.406
- [23] Idris Kabalci, Turgay Tay, Gönül Özen, Phys. Status Solidi., **C8**, 2625 (2011); https://doi.org/10.1002/pssc.201084089
- [24] Adam Strzęp, Michał Głowacki, Maksymilian Szatko, Karolina Potrząsaj, Radosław Lisiecki, Witold Ryba-Romanowski, J. Lumin., 116962 (2020); https://doi.org/10.1016/j.jlumin.2019.116962
- [25] H. Gebavi, D. Milanese, R. Balda, S. Chaussedent, M. Ferrari, J. Fernandez, M. Ferraris,
- J. Phys. D: Appl. Phys. 43, 135104 (2010); https://doi.org/10.1088/0022-3727/43/13/135104
- [26] Pavel Peterka, Ivan Kasik, Anirban Dhar, Bernard Dussardier, Wilfried Blanc, Opt. Express. 19, 2773 (2011); https://doi.org/10.1364/OE.19.002773
- [27] Meriam Tahenti, Noureddine Issaoui, Thierry Roisnel, Aleksandr S.
- Kazachenko, Maximiliano A. Iramain, Silvia Antonia Brandan, Omar Al-Dossary, Anna S. Kazachenko, Houda Marouani, Zeitschrift für Physikalische Chemie **237**, 1775 (2023); https://doi.org/10.1515/zpch-2023-0332
- [28] Yassine Slimani, Sher Singh Meena, Sagar E. Shirsath, Essia Hannachi, Munirah A. Almessiere, Abdulhadi Baykal, Rengasamy Sivakumar, Khalid M. Batoo, Atul Thakur, Ismail Ercan, Bekir Özçelik, Zeitschrift für Physikalische Chemie **237**: 1753 (2023); https://doi.org/10.1515/zpch-2023-0215
- [29] M. K. Halimah, M. F. Faznny, M. N. Azlan, H. A. Sidek. Results Phys. 7, 581(2017); https://doi.org/10.1016/j.rinp.2017.01.014
- [30] Heba Saudi, Ghada Adel. Optics. 6, 17 (2017)
- [31] C. Zaldo, Lanthanide-Based multifunctional materials, Chapter.10, Elsevier Inc., 10, 335 (2018);
- [32] Jag Mohan, Organic Spectroscopy, Narosa Publishing House, New Delhi (2000)

- [33] R. M. Silverstein, F. X. Webster, Spectrometric Identification of Organic compounds, 6th ed., John Wiley and Sons, USA (1991)
- [34] K.Nakamoto, Infrared and Raman Spectra of Inorganic and Coordination Compounds, John-Wiley and Sons. Inc., New York (1986)
- [35] M. Jackson, Magnetism of Rare Earth. The IRM quarterly 10, 3 (2000)
- [36] P. Sivaprakash, A. Nitthin Ananth, V. Nagarajan, R. Parameshwari, S. Arumugam, Sujin P. Jose, S. Esakki Muthu, Mater. Chem. Phys. **248**, 122922 (2020); https://doi.org/10.1016/j.matchemphys.2020.122922
- [37] P. Sivaprakash, K. AshokKumar, K. Subalakshmi, Chinna Bathula, Sanjay Sandhu, S. Arumugam, Mater. Lett. **275**, 128146 (2020); https://doi.org/10.1016/j.matlet.2020.128146 [38] S. Arumugam, P. Sivaprakash, A. Dixit, R. Chaurasiya, L. Govindaraj, Sci. Rep. **9**, 3200
- [38] S. Arumugam, P. Sivaprakash, A. Dixit, R. Chaurasiya, L. Govindaraj, Sci. Rep. 9, 3200 (2020); https://doi.org/10.1038/s41598-019-39083-8
- [39] Kunfeng Chen, Dongfeng Xue, J. Colloid Interface Sci. **424**, 84 (2014); https://doi.org/10.1016/j.jcis.2014.03.022
- [40] Yanhong Li, Liujun Cao, Lei Qiao, Ming Zhou, Yang Yang, Peng Xiao, Yunhuai Zhang, J. Mater. Chem. A **2**, 6540 (2014); https://doi.org/10.1039/C3TA15373H
- [41] Li Y, Peng H, Yang L, Dong H, Xiao P. J. Mater. Sci., **51**, 7108 (2016); https://doi.org/10.1007/s10853-016-9968-6
- [42] Xue-Feng Lu, Dong-Jun Wu, Run-Zhi Li, Qi Li, Sheng-Hua Ye, Ye-Xiang Tong, Gao-Ren Li, J. Mater. Chem. A 2, 4706 (2014); https://doi.org/10.1039/C3TA14930G
- [43] W. A. Badawy, M. M. El-Rabiei, N. H. Helal, H. M. Nady, Zeitschrift für Physikalische Chemie. **227**: 1143 (2013); https://doi.org/10.1524/zpch.2013.0347
- [44] Girish S. Gund, Deepak P. Dubal, Supriya B. Jambure, Sujata S. Shinde, Chandrakant D. Lokhande, J. Mater. Chem. A 1, 4793 (2013); https://doi.org/10.1039/C3TA00024A
- [45] B. A. Mei, O. Munteshari, J. Lau, B. Dunn, L.Pilon, J. Phys. Chem. C 122, 194 (2018); https://doi.org/10.1021/acs.jpcc.7b10582
- [46]https://partners.metrohm.com/GetDocumentPublic?action=get_dms_document&docid=20439
- [47] Woosung Choi, Heon-Cheol Shin, Ji Man Kim, Jae-Young Choi, Won-Sub Yoon, J. Electrochem. Sci. Technol. **11**, 1 (2020); https://doi.org/10.33961/jecst.2019.00528 [48] E. P. Randviir, C. E. Banks, Analy. Methods, **5**, 1098 (2013); https://doi.org/10.1039/C3AY26476A